Optical-lattice Hamiltonians for relativistic quantum electrodynamics

Eliot Kapit and Erich Mueller
Laboratory of Atomic and Solid State Physics, Cornell University, Ithaca, New York, USA
(Received 17 November 2010; published 28 March 2011)

We show how interpenetrating optical lattices containing Bose-Fermi mixtures can be constructed to emulate the thermodynamics of quantum electrodynamics (QED). We present models of neutral atoms on lattices in $1+1$, $2+1$, and $3+1$ dimensions whose low-energy effective action reduces to that of photons coupled to Dirac fermions of the corresponding dimensionality. We give special attention to $(2+1)$-dimensional quantum electrodynamics (QED3) and discuss how two of its most interesting features, chiral symmetry breaking and Chern-Simons physics, could be observed experimentally.

DOI: 10.1103/PhysRevA.83.033625 PACS number(s): 67.85.Pq, 11.15.Ha, 03.75.Lm

I. INTRODUCTION

Planar quantum electrodynamics (QED3) has been of great theoretical interest for many years. The restriction to lower dimensionality profoundly changes the structure of the electromagnetic field and its symmetries [1]. In two spatial dimensions ($2+1$ D), the electromagnetic potential between point charges scales as $\log r$ instead of r^{-1}, leading one to expect charge confinement in the appropriate limit. QED3 with massive fermions is particularly rich. One of the two possible Lorentz-invariant mass terms breaks parity and time-reversal symmetry, leading to a topological Chern-Simons term in the photon action. This term produces a gap in the photon spectrum and makes the effective interaction between the fermions short ranged. The other Lorentz-invariant fermion mass term breaks "chiral" symmetry and is spontaneously generated at low temperatures. Both confinement and chiral symmetry breaking occur in quantum chromodynamics; since QED3 is a much simpler theory, it has been studied as a model system for these effects [2–7]. Further, QED3 has been proposed as an effective theory for spin liquids [8,9] and the pseudogap phase of high-temperature superconductors [10–13]. A direct experimental realization of QED3 could therefore be relevant to many areas of both condensed-matter and high-energy physics.

Recent advances in cold-atom physics and optical lattices [14] have made the simulation of QED3 a real experimental possibility. Dirac fermions appear at half filling in a honeycomb optical lattice [15–19], mimicking the relativistic band structure of graphene [20]. They also appear in a square lattice with appropriate complex hopping matrix elements [21]. This has led to a number of proposals to emulate relativistic physics with cold atoms [21–29]. Here, we extend these previous proposals by showing how to emulate QED3 with cold atoms. By combining mixtures of bosons and fermions on interpenetrating optical lattices with appropriately tuned densities and interactions, both relativistic fermions and the full three-component dynamical gauge field can be constructed, allowing QED3 to be probed directly. The linear Bogoliubov excitations of three species of bosonic atoms correspond to the three components of the vector field A_μ. One of the boson species occupies the same lattice as the fermions, while the other two sit on alternating bonds between the fermion sites. These bosons modulate the fermion hopping amplitudes, leading to an interaction that at low energy has the form of a gauge coupling $e\overline{\psi}\gamma_\mu A_\mu \psi$. Being a lattice model, higher energy terms in this theory will naturally deviate from the emergent Lorentz and gauge invariances, but at low energies, these terms are heavily suppressed, and after applying the Wilsonian prescription of discarding irrelevant operators, the resulting Hamiltonian is that of QED3.

It is important to note that in the real-time formalism, the time (A_0) component of the gauge field is canonically quantized by operators with negative norm, with causality and Hermiticity preserved in real states by the Ward identity [30]. This is a general feature of vector bosons and cannot be duplicated with cold atoms. However, in the finite-temperature (imaginary-time) formalism, all the components of the A field have positive norm. Thus, we focus on producing a quantum simulator which reproduces the thermodynamics of QED3. Many of the most interesting properties of QED3 (such as mass generation and symmetry breaking) can be probed through equilibrium thermodynamics. Further, some real-time correlations can be accessed through the fluctuation-dissipation theorem.

Our construction is very different from traditional examples of gauge fields in condensed -matter systems [8–13,31]. Typically, these gauge theories arise from using descriptions with redundant degrees of freedom (such as slave bosons in the large-U Fermi-Hubbard model). The complicated underlying physics of these emergent gauge theories makes it difficult to use them as simulators of gauge physics itself. The approach that we take is different; instead of formulating a redundant description of a strongly interacting system, we take a weakly interacting system with a large number of degrees of freedom and tune the couplings and particle densities so that the low-energy physics is identical to thermal QED.

To construct our theory, we necessarily choose a particular gauge. The Hamiltonian of our theory is identical to that of QED in the Feynman gauge. Our theory is therefore not a true gauge theory in the formal sense of being described by an equivalence class of distinct actions and wave functions; rather, it is a theory of a relativistic fermion interacting with three neutral, independent massless bosons through a coupling of the form $\overline{\psi}\gamma_\mu A_\mu \psi$. All physical observables of QED are gauge independent, and despite its fixed gauge, our simulator should correctly reproduce all such observables.

The remainder of the paper is organized in the following manner. In Sec. II, we describe the canonical quantization

of QED3 in the Feynman gauge, taking care to denote the various terms in the Hamiltonian that must be replicated in our cold-atom system. In Sec. III, we then outline our model and show that its low-energy limit is identical to the Hamiltonian formulation of QED3. Following the derivation of our model, in Sec. IV we describe a series of experimental probes to study the more dramatic properties of QED3. Finally, in Secs. V – VII, we offer concluding remarks and discuss extensions of our theory to 1 + 1 and 3 + 1 dimensions.

II. QED AND GAUGE FREEDOM IN 2 + 1 DIMENSIONS

Our goal is to simulate the Euclidean action for (2 + 1)-dimensional quantum electrodynamics,

$$L_E = i\overline{\psi}\gamma_\mu\partial_\mu\psi + e\overline{\psi}\gamma_\mu A_\mu\psi - \tfrac{1}{4}F_{\mu\nu}F_{\mu\nu}. \tag{1}$$

We adopt the conventions that space-time indicies which run from 0 to 2 are represented by Greek letters and objects in boldface represent the two spatial components of the Lorentz three-vectors. Our imaginary time metric and γ matricies are

$$\begin{gathered} g_{\mu\nu} = -\delta_{\mu\nu}, \quad \overline{\psi} = i\psi^\dagger\gamma_0, \quad \gamma_0 = i\sigma_z, \\ \gamma_1 = i\sigma_x, \gamma_2 = i\sigma_y, \end{gathered} \tag{2}$$

and ψ is a two-component fermionic spinor. The σ_{xyz} are Pauli matricies, and $F_{\mu\nu} = \partial_\mu A_\nu - \partial_\nu A_\mu$ is the electromagnetic field strength tensor. Summation is implied for all repeated indicies, and we have abandoned the standard convention of raising and lowering indicies to emphasize that our imaginary-time metric is trivial. In Sec. III, we generalize this action to massive fermions. We work in the imaginary-time formalism [32,33] to ensure that the photon propagator $D_{\mu\nu}$ is positive definite, and therefore all photon states have positive norm and there are no ghostlike degrees of freedom. We note that in a non-Abelian theory, negative norm degrees of freedom will be found even in the imaginary-time formalism. Thus, our approach is not appropriate for simulating QCD.

We simulate this Hamiltonian by designing an optical-lattice system that exhibits identical degrees of freedom and Feynman rules up to lowest order in powers of momenta. To arrive at a simple enough form of the action for quantum simulation, we employ the Faddeev-Popov gauge-fixing procedure [30]. This scheme enforces the gauge constraint

$$\partial_\mu A_\mu = w(x) \tag{3}$$

and then path integrates over w to remove the gauge degrees of freedom from the Lagrangian. So long as we restrict ourselves to calculating only gauge-invariant quantities, the integration over w can be performed trivially. This alters the Euclidean action by adding a term of the form

$$L_E \to L_E - \frac{1}{2\xi}(\partial_\mu A_\mu)^2, \tag{4}$$

where ξ is an arbitrary parameter. If we then choose $\xi = 1$ (the Feynman gauge), the off-diagonal terms in the photon propagator cancel out, and we are left with the action

$$L_E = i\overline{\psi}\gamma_\mu\partial_\mu\psi + e\overline{\psi}(\gamma_\mu A_\mu)\psi + \tfrac{1}{2}\partial_\mu A_\nu\partial_\mu A_\nu. \tag{5}$$

Within this gauge, our system is described by the Hamiltonian

$$H = v_F\overline{\psi}(\overrightarrow{\sigma}\cdot\mathbf{k})\psi + e\overline{\psi}(\sigma_z A_0 + i\overrightarrow{\sigma}\cdot\mathbf{A})\psi + \tfrac{1}{2}\partial_\nu A_\mu\partial_\nu A_\mu, \tag{6}$$

$$\frac{1}{2}\partial_\nu A_\mu\partial_\nu A_\mu = \sum_{r=0}^{2}\sum_{\mathbf{k}}\omega_{\mathbf{k}}\alpha^\dagger_{r\mathbf{k}}\alpha_{r\mathbf{k}}.$$

The α_r operators annihilate a photon of polarization r, and $\omega_{\mathbf{k}} = v_s|k|$; this is simply the canonical quantization of the free-photon Hamiltonian. Note that, unlike in Minkowski space, $[\alpha_{r\mathbf{k}},\alpha^\dagger_{s\mathbf{p}}] = \delta_{rs}\delta^2(\mathbf{k}-\mathbf{p})$ describes only positive norm states, since the negative time-time component of the photon propagator is made positive by the rotation to imaginary time. The gauge field A is quantized in terms of these bosons by

$$A_\mu(\mathbf{x}) = \sum_{r=0}^{2}\sum_{\mathbf{k}}\frac{f_{r\mathbf{k}\mu}}{\sqrt{2\omega_{\mathbf{k}}}}[\alpha_{r\mathbf{k}}e^{i\mathbf{k}\cdot\mathbf{x}} + \alpha^\dagger_{r\mathbf{k}}e^{-i\mathbf{k}\cdot\mathbf{x}}]. \tag{7}$$

Here, the $f_{r\mathbf{k}\mu}$ are real, three-element polarization vectors satisfying $f_{r\mathbf{k}}\cdot f_{s\mathbf{k}} = \delta_{rs}$. The Ward identity [34] implies that real photons are transverse, that is, $\mathbf{k}\cdot\mathbf{f}_{s\mathbf{k}} = 0$ for all physical states; only transverse photons will be produced or destroyed in observable processes. The momentum-space propagators for the fermion and gauge field are

$$D_F = \frac{-1}{\gamma_\mu k^\mu + m + i\epsilon}, \quad D_{\mu\nu} = \frac{-\delta_{\mu\nu}}{k^2 + i\epsilon}. \tag{8}$$

We now show how cold atoms can be used to directly implement the Hamiltonian (6).

III. (2 + 1)-DIMENSIONAL OPTICAL-LATTICE QED

We give two alternative geometries for the lattice confining our fermions. We require that the system exhibits "Dirac points" instead of a Fermi surface; all zero- or low-energy fermionic excitations must occur near some finite set of points $\mathbf{K}$ in momentum space and have the dispersion relation $\epsilon_{\mathbf{p}} = \pm\sqrt{v_F^2\mathbf{p}^2 + m^2}$ for small $\mathbf{p}$ measured with respect to $\mathbf{K}$. The most well-known system of this type is the honeycomb lattice [15–19], realized in condensed matter in graphene [20] and carbon nanotubes. In cold atoms, the ability to directly manipulate the phases of lattice hopping amplitudes enables the creation of Dirac points in a square lattice [21,26–29], something that has not been realized in materials. We describe both approaches.

A. Square-lattice implementation

Our square-lattice approach is based on the geometry proposed by Liu *et al.* [21] to study the anomalous quantum Hall effect. Consider noninteracting fermions in an square optical lattice with nearest neighbor hopping t and lattice spacing l. We add to the hopping amplitude a set of phases such that

$$\begin{aligned} H &= -\sum_{jk} t_{jk}\psi^\dagger_j\psi_k; \\ t_{jk} &= t\ \{y_j = y_k\}(\text{horizontal hop}), \\ &= it{-}1^{x_j+y_j}\ \{y_j \neq y_k\}(\text{vertical hop}). \end{aligned} \tag{9}$$

The operators ψ_j and $\psi_j^\dagger$ destroy or create a fermion at site j. This structure is mathematically identical to a constant magnetic field with flux density π (or half of a fundamental magnetic flux quantum ϕ_0) per plaquette. This effective magnetic field could be realized through a spatially dependent Raman coupling to an external laser field [35–38].

To find the band structure, we break the lattice into two sublattices R and S, depending on whether $x_j + y_j$ is even or odd (Fig. 1). The momentum space Hamiltonian can be written as the dot product of a pair of two-component spinors through a matrix. This matrix M has no diagonal elements because nearest neighbor hopping always transfers a fermion between sublattices,

$$H_D = -2t \sum_{\mathbf{k}} \{\psi_{R\mathbf{k}}^\dagger, \psi_{S\mathbf{k}}^\dagger\} \cdot M \cdot \{\psi_{R\mathbf{k}}, \psi_{S\mathbf{k}}\},$$
$$M = \begin{pmatrix} 0 & \cos k_x l + i \cos k_y l \\ \cos k_x l - i \cos k_y l & 0 \end{pmatrix}. \tag{10}$$

This Hamiltonian produces a Dirac cone dispersion about the four $\mathbf{K}$ points $\mathbf{K}_{\pm\pm} = \{\pm\pi/2l, \pm\pi/2l\}$. Only two of these points ($\mathbf{K}_{++}$ and $\mathbf{K}_{+-}$) are distinct; the others are related to them by symmetry. We predominantly focus on $\mathbf{K}_{++} = \pi/2l\,\{1,1\} = \mathbf{K}$ and let $\mathbf{k} = \mathbf{K} + \mathbf{p}$; the structure at the other $\mathbf{K}$ point is the same up to the signs of the Dirac γ matricies. With the definitions (2), small $\mathbf{p}$ and $\psi_{\mathbf{p}} = \{\psi_{R\mathbf{p}}, \psi_{S\mathbf{p}}\}$, our Hamiltonian becomes

$$H_D = 2tl \sum_{\mathbf{p}} \psi_{\mathbf{p}}^\dagger \begin{pmatrix} 0 & p_x + ip_y \\ p_x - ip_y & 0 \end{pmatrix} \psi_{\mathbf{p}}$$
$$= 2tl \sum_{\mathbf{p}} \overline{\psi}_{\mathbf{p}} (\gamma \cdot \mathbf{p}) \psi_{\mathbf{p}}, \tag{11}$$

We now add a gauge field to the theory by introducing three species of lattice bosons. One of the three boson species (a_0) lives on the same lattice as the fermions, and the other two (a_1 and a_2) occupy interpenetrating square lattices as shown in Fig. 1. If the interaction between the bosons and fermions is repulsive, the presence of a_1 bosons between a pair of neighboring fermion lattice sites acts as an effective potential barrier that reduces the hopping amplitude between the two sites. Similarly, the presence of the fermions will modulate the boson hopping and lead to a nearest neighbor repulsion term between bosons and fermions. The total Hamiltonian incorporating all of these effects is

$$\{\mathbf{x} \in L_f, \mathbf{y}_{b=1,2} \in L_{b=1,2}\}$$
$$H = -t \sum_{\mathbf{x},\mathbf{s}} \psi_{R/S\mathbf{x}}^\dagger \psi_{S/R\mathbf{x}\pm\mathbf{s}} e^{i\phi_{\mathbf{x},\mathbf{s}}} + \sum_{b;\mathbf{k}} \epsilon_{b\mathbf{k}} a_{b\mathbf{k}}^\dagger a_{b\mathbf{k}} + \sum_{\mathbf{x};b} \frac{V_b}{2} n_{b\mathbf{y}_b}(n_{b\mathbf{y}_b} - 1) + g_0 \sum_{\mathbf{x}} \psi_{\mathbf{x}}^\dagger \psi_{\mathbf{x}} n_{0\mathbf{x}}$$
$$+ \sum_{b=1,2;\mathbf{x},\mathbf{s}} g_b \psi_{R/S\mathbf{x}}^\dagger \psi_{S/R\mathbf{x}\pm\mathbf{s}} n_{b\mathbf{y}_b=\mathbf{x}\pm\frac{\mathbf{s}}{2}} + \sum_{b;\mathbf{x}} g_b n_{b\mathbf{y}_b} \psi_{R/S\mathbf{x}}^\dagger \psi_{R/S\mathbf{x}} + \sum_{b=1,2;\mathbf{y}} g_b' a_{b\mathbf{y}_b\pm 2\mathbf{s}}^\dagger a_{b\mathbf{y}_b} \psi_{R/S\mathbf{x}=\mathbf{y}_b\pm\frac{\mathbf{s}}{2}}^\dagger \psi_{R/S\mathbf{x}=\mathbf{y}_b\pm\frac{\mathbf{s}}{2}}. \tag{12}$$

The sum over b is over boson flavors (either 0, 1, 2 or 1, 2 as specified), and the vector $\mathbf{s}$ joins nearest neighbors and is equal to $(\pm l\hat{x},0),(0,\pm l\hat{y})$, where, as previously defined, l is the lattice spacing. L_f is the fermion lattice, and L_b is the lattice associated with species b. The operator $n_{b\mathbf{y}}$ measures the density of a_b particles at $\mathbf{y}$. From left to right, the terms on the first line are the fermion hopping term, the boson kinetic terms $\epsilon_{b\mathbf{k}}$ (which include the boson chemical potentials), the weak repulsive contact interaction V_b between bosons, and the local repulsion between fermions and the a_0 bosons. The terms on the second line are the boson mediation of fermion hopping, nearest neighbor Bose-Fermi repulsion, and fermion mediation of boson hopping. We assume that there are no direct interactions between bosons of different species as they are spatially separated. The g_b are the effective interactions between the bosons and fermions, which can be tuned by manipulating the optical potential depth or through Feshbach resonances and are calculated from the overlap of the neighboring Wannier functions [39]. For simplicity, we assume that $g_b = g_b'$, a situation that we expect can be reached through appropriate fine-tuning. In the tight-binding limit, next nearest neighbor hopping and any additional interactions are vanishingly small. The last two terms in Eq. (12) can lead to unwanted terms in our low-energy action. As calculated below, their contributions cancel each other if the $b = 1,2$ bosons are condensed about $\mathbf{K} = \{\pi/2l,\pi/2l\}$. This can be engineered, for example, by using the techniques of Ref. [36]

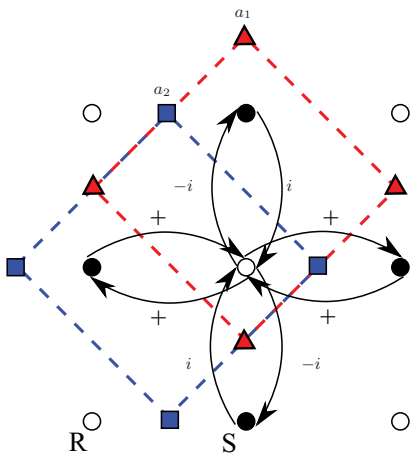

FIG. 1. (Color online) Square lattice for QED3. The fermions are confined to the lattice sites R and S, denoted by white and black circles. The bosons sit on the red triangles and blue squares denoted by α_1 and α_2. Overall phases for fermion hopping are labeled in the figure.

to introduce phases on the hopping matrix elements. Under these conditions,

$$\epsilon_{b=1,2\mathbf{k}} = +2t_{b=1,2}\left(\cos\frac{\mathbf{k}_x}{2l} + \cos\frac{\mathbf{k}_y}{2l} - \mu_b\right),$$
$$\epsilon_{0\mathbf{k}} = -2t_0\left(\cos\frac{\mathbf{k}_x}{l} + \cos\frac{\mathbf{k}_y}{l}\right) - \mu_0, \tag{13}$$

where the t_b are positive numbers parametrizing the boson hopping. We now show that, with appropriate choices for the various parameters, the low-energy excitations of Eq. (12) are exactly those of QED3.

We first assume that the temperature is low enough that all of the boson fields have condensed; if this is the case, we can expand the Bose operators around the condensate expectation values, dropping terms that are quadratic or higher in boson fluctuations. For example, if $b = 1,2$,

$$n_{b\mathbf{x}} = n_b + \sqrt{n_b}(-1)^{x+y}(\widehat{a}^\dagger_{b\mathbf{x}} + \widehat{a}_{b\mathbf{x}}) + O\left(\frac{1}{n}\right)$$
$$\equiv n_b + \sqrt{n_b}(-1)^{x+y}G_{b\mathbf{x}}, \tag{14}$$

where $\widehat{a}_{b\mathbf{x}} = a_{b\mathbf{x}} - \sqrt{n_b}$. To treat the bosons' self-interactions and vacuum expectation value, we perform a Bogoliubov transformation [40]. For a given species, this process gives

$$H_b = \sum_{\mathbf{k}} E_{b\mathbf{k}}\alpha^\dagger_{b\mathbf{k}}\alpha_{b\mathbf{k}}, \quad E_{b\mathbf{k}} = \sqrt{\epsilon_{b\mathbf{k}}(\epsilon_{b\mathbf{k}} + 2n_bV_b)},$$
$$\widehat{a}_{b\mathbf{k}} = u_{b\mathbf{k}}\alpha_{b\mathbf{k}} - v_{b\mathbf{k}}\alpha^\dagger_{b-\mathbf{k}}.$$

Here, $u_{b\mathbf{k}}$ and $v_{b\mathbf{k}}$ are real constants satisfying $u^2_{\mathbf{k}} - v^2_{\mathbf{k}} = 1$,

$$u_{b\mathbf{k}} = \sqrt{\frac{\epsilon_{b\mathbf{k}} + n_bV_b}{E_{b\mathbf{k}}} + \frac{1}{2}}, \quad v_{b\mathbf{k}} = -\sqrt{\frac{\epsilon_{b\mathbf{k}} + n_bV_b}{E_{\mathbf{k}_b}} - \frac{1}{2}}. \tag{15}$$

Furthermore, at low momenta these coherence factors simplify,

$$\lim_{\mathbf{k}\to 0} u_{\mathbf{k}} = -\lim_{\mathbf{k}\to 0} v_{\mathbf{k}} = \sqrt{nV/E_{\mathbf{k}}}, \tag{16}$$

allowing us to use the low-energy approximation

$$G_{b\mathbf{k}} \approx 2\sqrt{n_b\frac{V}{E_{\mathbf{k}}}}[\alpha_{b\mathbf{k}} + \alpha^\dagger_{b-\mathbf{k}}]. \tag{17}$$

The "speed of light" for these bosons is $v_b = \sqrt{n_bV_b/m_b}$. We tune the t_b so that the Fermi velocity v_F matches each of the three v_b.

Now consider the first term on the second line of Eq. (12). Expanding the fields in momentum space and summing over $\mathbf{k}$ and b yields

$$\sum_{b=1,2;\mathbf{x}} g_b\psi^\dagger_{R/S\mathbf{x}}\psi_{S/R\mathbf{x}\pm\mathbf{l}}n_{b\mathbf{x}\pm\mathbf{l}_b/2}$$
$$= +\sum_{b=1,2,\mathbf{k},\mathbf{p},\mathbf{q}} \sqrt{n_b}g_b(G_{b\mathbf{k}}\overline{\psi}^\dagger_{\mathbf{p}}\gamma_b\psi_{\mathbf{q}})\delta_{\mathbf{k}+\mathbf{p}-\mathbf{q}}$$
$$+\sum_{b=1,2;\mathbf{k}} g_bn_b(\overline{\psi}^\dagger_{\mathbf{k}}\gamma_b\psi_{\mathbf{k}}) + O\left(\frac{1}{n},l\mathbf{k},l\mathbf{p},l\mathbf{q}\right). \tag{18}$$

Here, the momenta in G and ψ are expanded about $\{\pi/2l,\pi/2l\}$ and $\mathbf{K}$, respectively. Similarly, the local repulsion term adds two terms of the form

$$g_0\sum_{\mathbf{x}}\psi^\dagger_{\mathbf{x}}\psi_{\mathbf{x}}n_{0\mathbf{x}} = n_0g_0\sum_{\mathbf{k}}\overline{\psi}_{\mathbf{k}}\gamma_0\psi_{\mathbf{k}}$$
$$+ g_0\sqrt{n_0}\sum_{\mathbf{k},\mathbf{p},\mathbf{q}}(G_{0\mathbf{k}}\overline{\psi}^\dagger_{\mathbf{p}}\gamma_0\psi_{\mathbf{q}})\delta_{\mathbf{k}+\mathbf{p}-\mathbf{q}}$$
$$+ O\left(\frac{1}{n},l\mathbf{k},l\mathbf{p},l\mathbf{q}\right). \tag{19}$$

We can account for the remaining two terms on the second line of (12) through a similar expansion. Assuming that $g_b = g'_b$, we find that with our choice of boson dispersion (with a minimum at $\{\pi/2l,\pi/2l\}$) these two terms precisely cancel each other to lowest order in $\mathbf{k}$. No such cancellation occurs if the bosons are condensed about $\mathbf{k} = 0$. The resulting low-energy theory is

$$H = v_F\sum_{\mathbf{k}}\overline{\psi}_{\mathbf{k}}\gamma\cdot\mathbf{k}\psi_{\mathbf{k}} + \sum_{b=0}^{2}\sum_{\mathbf{k}}\omega_{\mathbf{k}}\alpha^\dagger_{b\mathbf{k}}\alpha_{b\mathbf{k}}$$
$$+\sum_{b=0}^{2}\sum_{\mathbf{k},\mathbf{p}} g_b(\sqrt{n_b}G_{b\mathbf{k}} + n_b)\overline{\psi}_{\mathbf{p}}\gamma_b\psi_{\mathbf{k}+\mathbf{p}}$$
$$+ O\left(\frac{1}{n},l\mathbf{k},l\mathbf{p},l\mathbf{q}\right). \tag{20}$$

Comparing $G_{b\mathbf{k}}$ in (17) to the canonical quantization of the gauge field A in (7) leads us to write

$$G_{b\mathbf{x}} = 2\sqrt{2n_bV_b}A_{b\mathbf{x}}. \tag{21}$$

Provided that $v_b = \sqrt{n_bV_b/m_b} = v_F$ and $2n_b\sqrt{2V_b}g_b = e$ for all three boson species, we finally see that (20) reduces to (6) with the addition of a constant shift of the gauge

$$\overline{\psi}\gamma_\mu A_\mu\psi \to \overline{\psi}\gamma_\mu(A_\mu + B_\mu)\psi, \quad B_\mu = \frac{1}{\sqrt{V_b}}. \tag{22}$$

This constant shift has no effect on the overall physics of the theory and simply shifts the location of the Dirac points in $\mathbf{k}$ space.

For K^{40} fermions and Rb^{87} fermions with a lattice depth of $4E_R$ (where E_R is the recoil energy) for each lattice, an average boson density of unity, and a Bose-Fermi scattering length of $-177a_0$ [41], the coupling constant e (in units of square root temperature) is approximately 2 $nK^{1/2}$. This value can be tuned considerably through Feshbach resonances, optical-lattice tuning, and adjusting the boson filling.

B. Honeycomb lattice

Our theory can also be realized on a honeycomb optical lattice [15–20]. Assume that the spacing between vertices in the hexagons is l. The basis vectors δ connecting a pair of nearest neighbor sites are

$$\delta_1 = \left(\frac{-l}{\sqrt{3}},0\right), \quad \delta_2 = \left(\frac{l}{2\sqrt{3}},-\frac{l}{2}\right), \quad \delta_3 = \left(\frac{l}{2\sqrt{3}},\frac{l}{2}\right). \tag{23}$$

After dividing the lattice into two triangular sublattices R and S (see Fig. 2), we arrive at the fermion hopping Hamiltonian

$$H = -t \sum_{\mathbf{k}} \sum_{j=1}^{3} [e^{i\mathbf{k}\cdot\delta_j} \psi^{\dagger}_{R\mathbf{k}} \psi_{S\mathbf{k}} + \text{H.c.}]. \tag{24}$$

The coefficients $\sum_{j=1} e^{i\mathbf{k}\cdot\delta_j}$ vanish at six points $\mathbf{K}$, of which only two are unique—the other four are related by reciprocal lattice vectors. We choose $\mathbf{K}_{\pm} = \pm\frac{2\pi}{l}(0, \frac{2}{3})$. For small $\mathbf{k}$ defined relative to one of these two $\mathbf{K}$ points, the Hamiltonian is the familiar Dirac cone:

$$H_D = \frac{tl\sqrt{3}}{2} i\overline{\psi}\overrightarrow{\sigma} \cdot \mathbf{k}\psi. \tag{25}$$

As in the previous section, $\psi = \{\psi_R, \psi_S\}$ is a two-component spinor and $\overline{\psi} = \psi^{\dagger}\gamma_0$. We again construct the gauge field by adding three BEC fields, as shown in Fig. 2. The boson a_0 sits on the same lattice as the fermions, but a_1 and a_2 are instead on the links between the fermion lattice sites. Specifically, a_1 is chosen to occupy sites separated by δ_1 and δ_2, and a_2 occupies sites separated by δ_1 and δ_3. This structure breaks the C_6 symmetry of the lattice, but if the coefficients are chosen properly, the low-energy theory will be rotationally invariant. As in the square-lattice case, we require that the hopping matrix elements for b_1 and b_2 to be opposite in sign to those of b_0. This will again allow the unwanted nearest neighbor repulsion and fermion mediation of boson hopping to cancel each other. Ignoring these terms, we are left with

$$H_{\text{int}} = \sum_{\mathbf{x}} \left[g_{\delta_1} \psi^{\dagger}_{R\mathbf{x}} \psi_{S\mathbf{x}+\delta_1} \left(n_{1\mathbf{x}+\frac{\delta_1}{2}} + n_{2\mathbf{x}+\frac{\delta_1}{2}} \right) + g_{\delta_2} \psi^{\dagger}_{R\mathbf{x}} \psi_{S\mathbf{x}+\delta_2} n_{1\mathbf{x}\frac{\delta_2}{2}} + g_{\delta_3} \psi^{\dagger}_{R\mathbf{x}} \psi_{S\mathbf{x}+\delta_3} n_{2\mathbf{x}\frac{\delta_3}{2}} + \text{H.c.} \right]. \tag{26}$$

The couplings g are determined from the fermion-boson scattering amplitudes and from the geometric position of the bosons relative to the fermion lattice sites.[1] Repeating the steps in Eqs. (14)–(20) and setting

$$g_{\delta_2} = g_{\delta_3} = g, g_{\delta_1} = \tfrac{1}{2}(1 + \sqrt{3})g \tag{27}$$

yields the QED Hamiltonian (6) with an effective charge $e = 2\sqrt{3Vng}$ and a speed of light $v_F = tl\sqrt{3}/2$.

[1]For example, one could reduce these amplitudes by staggering some of the boson lattice sites in the z direction out of the plane.

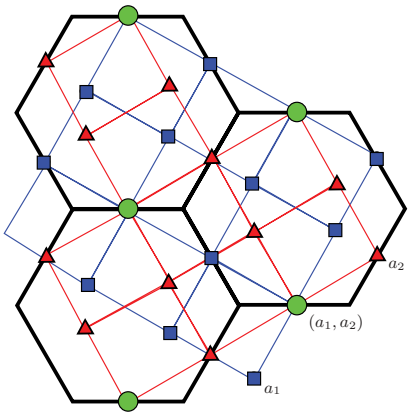

FIG. 2. (Color online) Honeycomb optical lattice for QED3. The fermions and a_0 bosons sit on the vertices of the honeycomb lattice (in black). The two other boson species a_1 and a_2 are on the interpenetrating orthorhombic lattices (a_1 bosons are confined to the blue squares, a_2 bosons are confined to the red triangle), and the green circles indicate sites shared by the two lattices. The hopping parameters of these lattices can be tuned so that the low-energy dispersion $\epsilon_{\mathbf{k}}$ is simply $\mathbf{k}^2/2m^*$ for each of the three species.

IV. EXPERIMENTAL PROBES OF QED3

The successful realization of our QED3 simulator in an optical lattice would allow for a number of interesting experiments to study the properties of QED3. In this section, we outline three of these properties and propose experiments to measure them. (A) We describe the consequences of real and virtual photon polarizations. (B) At low temperatures, massless QED3 undergoes a phase transition to massive fermions. In our simulator, this phase transition leads to a spontaneous charge density wave, and we outline probes of this charge density wave order. (C) We describe an experiment which generates a topological photon mass (Maxwell-Chern-Simons electrodynamics), an effect only possible in $2 + 1$ dimensions. We demonstrate how an alteration of the fermion lattice could lead to such a term and show how it could be measured through two-photon Bragg scattering or rf spectroscopy. (D) Finally, we discuss the stability of QED3 against experimental inhomogenieties and perturbations, and demonstrate that perturbations which preserve the emergent Lorentz and gauge symmetries can be ignored.

A. Physical and virtual photons

An important property of QED3 is the fact that there is only a single physical polarization for the photon. This means that in any experiment neither timelike nor longitudinal photons can be created or destroyed. Consequently, in our emulation of QED3, no perturbation of the fermions will produce these "unphysical" photons. This is a dramatic observable, and one which could be studied through the introduction of optical perturbations which act on the fermions but which would leave the bosons unchanged in the absence of the Fermi-Bose interaction.

B. Spontaneous symmetry breaking and density wave order

At sufficiently low temperatures, thermal QED3 is expected to undergo a phase transition to a state with broken chiral

symmetry and a finite fermion mass [2–7,42–44]. Chiral symmetry relates the two Dirac points of our lattice model, and as we show below, chiral symmetry breaking on our square lattice corresponds to a commensurate $\{\pi,\pi\}$ charge density wave. A number of experimental techniques have been developed to measure density waves in optical lattices. Chief among these is light scattering [45], a cold-atom analog of the Bragg scattering of x rays or neutrons in solid-state materials. Alternately, the density wave order could be detected through *in situ* imaging of the cloud density [46].

To understand the origin of chiral symmetry breaking and its subsequent manifestation as a density wave order, we must first define the chiral symmetry itself. We choose a new notation to combine the fermions at the two Dirac points into a single four-component Dirac spinor. Defining $\mathbf{k} = \mathbf{K}_\pm + \mathbf{p}$, we write

$$\begin{gathered} H = i\overline{\psi}(\Gamma\cdot\mathbf{p}),\psi, \\ \psi_{\mathbf{p}} = \{\psi_{R\mathbf{K}_+ +\mathbf{p}},\psi_{S\mathbf{K}_+ +\mathbf{p}},\psi_{R\mathbf{K}_- +\mathbf{p}},\psi_{S\mathbf{K}_- +\mathbf{p}}\}, \\ \Gamma_0 = \begin{pmatrix}\sigma_z & 0\\ 0 & \sigma_z\end{pmatrix},\quad \Gamma_x = \begin{pmatrix}\sigma_x & 0\\ 0 & \sigma_x\end{pmatrix}, \\ \Gamma_y = \begin{pmatrix}\sigma_y & 0\\ 0 & -\sigma_y\end{pmatrix}. \end{gathered} \tag{28}$$

The photon coupling becomes $e\overline{\psi}\Gamma_\mu A_\mu\psi$, and we have simply obtained a larger representation of the Dirac algebra. This theory is invariant under transformations of the form

$$\psi \to \exp(i\epsilon_1 C_1)\exp(i\epsilon_2 C_2)\psi, \tag{29}$$

for any real constants ϵ_1 and ϵ_2 and 4×4 chiral matricies C_1 and C_2 defined by

$$C_1 = \begin{pmatrix}0 & \sigma_y\\ \sigma_y & 0\end{pmatrix},\quad C_2 = i\begin{pmatrix}0 & -\sigma_y\\ \sigma_y & 0\end{pmatrix}. \tag{30}$$

These matrices anticommute with each other and with all three Γ matrices. They are the generators of a symmetry transformation that simultaneously flips between the two sublattices and the two $\mathbf{K}_\pm$ points.

As described in detail in [2–7,42–44], the vacuum structure of (naively massless) QED3 at low temperature is nontrivial and spontaneously breaks this symmetry. This manifests as a vacuum expectation value $\langle\sum_k \bar{\psi}_k\psi_k\rangle \neq 0$. In the variables of our real-space lattice, this order parameter is a charge density wave of the form

$$\left\langle\sum_k \bar{\psi}_k\psi_k\right\rangle = \sum_{\mathbf{x}\in L_S}\psi^\dagger_{S\mathbf{x}}\psi_{S\mathbf{x}} - \sum_{\mathbf{x}\in L_R}\psi^\dagger_{R\mathbf{x}}\psi_{R\mathbf{x}}, \tag{31}$$

where R and S are the two fermionic sublattices. As previously emphasized, this order can be observed using light scattering or through single-site imaging of the fermions. Unfortunately, the transition temperature for this spontaneous symmetry breaking is $T_c \sim 10^{-2}e^2$ [6,47]. Using our previous estimate $e \sim 3\ (\mathrm{nK})^{1/2}$, we find that $T_c \sim 100$ pK is beyond the reach of current experiments. However, the Bose-Fermi interaction could potentially be increased through Feshbach resonances, pushing T_c to higher values.

C. Construction and probes of a topological photon mass

For many reasons, electrodynamics in $2+1$ dimensions is richer than its $(3+1)$-dimensional manifestation. One of the most dramatic effects of this dimensional reduction is the possibility of a topological photon mass, or Chern-Simons term [1–3,48–50], which both alters the structure of gauge invariance in the theory and opens an excitation gap to the creation of photons. Below, we describe how to generate this term through the addition of next nearest neighbor hopping to the fermions and suggest probes to detect the resulting photon mass.

In $2+1$ dimensions, there are two linearly independent, Lorentz-invariant terms which lead to a massive fermion dispersion relation $\omega = \sqrt{v_F^2\mathbf{k}^2 + m_0^2 + m_c^2}$,

$$H_m = m\sum_{\mathbf{k}}\overline{\psi}_{\mathbf{k}}\psi_{\mathbf{k}},\quad H_C = im_C\sum_{\mathbf{k}}\overline{\psi}_{\mathbf{k}}C_1C_2\psi_{\mathbf{k}}. \tag{32}$$

The first, H_m, breaks chiral symmetry and can be experimentally engineered by introducing a superlattice potential. In terms of the original fermionic sublattices R and S, we can write H_m as

$$H_m = m\left[\sum_{\mathbf{x}\in L_S}\psi^\dagger_{S\mathbf{x}}\psi_{S\mathbf{x}} - \sum_{\mathbf{x}\in L_R}\psi^\dagger_{R\mathbf{x}}\psi_{R\mathbf{x}}\right]. \tag{33}$$

This term leaves the photon modes qualitatively unchanged and, as explained in the previous section, generates an experimentally measurable density wave.

The chiral mass term H_C is more interesting, as it has dramatic consequences for the photons. In the presence of chiral-massive fermions, the resummation of one-loop corrections to the photon propagator introduces a Chern-Simons term [1] in the action of the form

$$L_{\mathrm{CS}} = \frac{\Delta}{4}A_\beta F_{\alpha\gamma}\epsilon_{\alpha\beta\gamma}, \tag{34}$$

with $\Delta \sim m_C$. This term is not found in $(3+1)$-dimensional theories. Further, there is no transition temperature above which $\Delta = 0$ (although the value of Δ does tend to decrease with increasing T), making it more experimentally accessible than the chiral symmetry breaking of the previous section. Within the Feynman gauge, the Chern-Simons term (34) yields a modified photon propagator:

$$D_{A\mu\nu} = \frac{-1}{p^2+|\Delta|^2}\left(\delta_{\mu\nu} - \frac{p_\mu p_\nu - i\Delta\epsilon_{\mu\nu\alpha}p_\alpha}{p^2}\right) - \frac{p_\mu p_\nu}{p^4} \tag{35}$$

with a photon mass gap $|\Delta|$. The action L_{CS} is only gauge invariant up to a boundary term, reducing the symmetry of the system to a subset of all possible gauge transformations. The properties of QED3 with a chiral mass term are therefore sensitive to the topology of the $(2+1)$-dimensional space.

Surprisingly, the requisite chiral fermion mass is straightforward to implement. In terms of the two sublattice fermion operators, the chiral mass term H_C is

$$\begin{aligned} H_C = m_C\sum_{\mathbf{p}}(&\psi^\dagger_{R\mathbf{K}_+ +\mathbf{p}}\psi_{R\mathbf{K}_+ +\mathbf{p}} - \psi^\dagger_{S\mathbf{K}_+ +\mathbf{p}}\psi_{S\mathbf{K}_+ +\mathbf{p}} \\ &- \psi^\dagger_{R\mathbf{K}_- +\mathbf{p}}\psi_{R\mathbf{K}_- +\mathbf{p}} + \psi^\dagger_{S\mathbf{K}_- +\mathbf{p}}\psi_{S\mathbf{K}_- +\mathbf{p}}). \end{aligned} \tag{36}$$

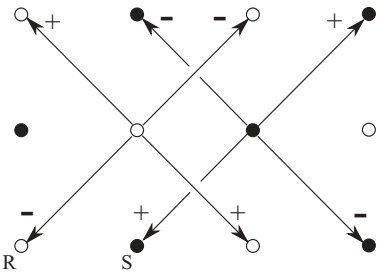

FIG. 3. Hopping terms that lead to a chiral mass H_C. The phase factors of (± 1) are labeled in the figure; the phase of a hopping term changes sign when rotated by $\pi/4$ and between sublattices R and S for the same direction. These phases correspond to a virtual magnetic flux of π per plaquette (half a flux quantum). Since this virtual flux was already introduced to create the Dirac fermions, a chiral mass could be introduced simply through allowing next nearest neighbor hopping.

H_C is invariant under a transformation which simultaneously switches the two sublattices and rotates between the two **K** points but is not invariant under either transformation individually. The simplest perturbation which obeys this symmetry is a next nearest neighbor hopping term with direction-dependent phases, shown in Fig. 3. The Hamiltonian for this term is

$$H_{\mathrm{NNN}} = \frac{m_C}{4} \sum_{\mathbf{x},j} (-1)^{x+y} (-1)^j \psi^\dagger_{R/S\mathbf{x}} \psi_{R/S\mathbf{x}+\mathbf{s}_j}, \qquad (37)$$

where the four $\mathbf{s}_j$ vectors join a site and its next nearest neighbors. The phases of these hopping terms change sign under a $\pi/4$ rotation and between the two sublattices R and S. Such hopping phases are natural in our model, Eq. (12), where the fermions experience an effective magnetic flux of π per plaquette: The phases correspond to a flux of $\pi/2$ through each triangular half-plaquette. To lowest order in $\mathbf{p}$, H_{NNN} reduces to H_C. Tuning the lattice to allow nearest neighbor hopping would therefore introduce a chiral mass gap into the model.

Engineering this chiral mass in our optical lattice would allow us to study Maxwell-Chern-Simons electrodynamics [1–3,48–50]. As seen in Eq. (35), there will be a gap in the photon spectrum. Since the photon in our model can be identified with excitations about a BEC, this photon mass implies the existence of a neutral Bose condensate with a gapped spectrum. This unusual spectral feature could be detected through rf spectroscopy [51] or through its thermodynamic consequences. The most effective probe, however, would likely be two-photon Bragg scattering [52–54]. This technique has been used to probe the dispersion $\epsilon_{\mathbf{k}}$ and coherence factors of the Bogoliubov quasiparticles of a BEC and thus would be able to directly measure the photon mass gap.

Another interesting property of the chiral fermion mass is its potential relationship to phenomena in theories of high-temperature superconductivity. Given that p in Eq. (36) is small compared to $\mathbf{K}_\pm$, one can write, in terms of the d-density wave operator Θ,

$$H_c \simeq 2m_c \sum_{R,S} \psi^\dagger_{R/S\mathbf{k}+\{\pi/l,\pi/l\}} \psi_{R/S\mathbf{k}} \sin 2\theta_{\mathbf{k}} = 2m_c \Theta, \qquad (38)$$

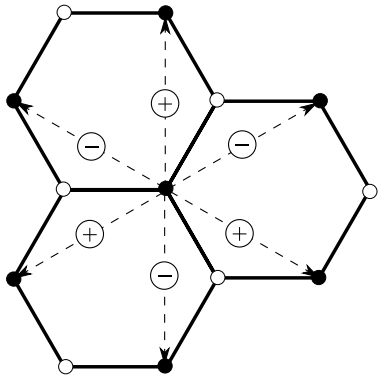

FIG. 4. The signs of the hopping amplitudes in Eq. (39) for a given sublattice in the honeycomb lattice. All signs are reversed for hopping within the other sublattice. Properly implemented, this term yields a chiral mass and will create gaps in the spectra of the three BEC fields.

where $\tan(\theta_{\mathbf{k}}) = k_y/k_x$. Several authors, including Chakravarty *et al.* [55], have proposed that such d-density wave order plays a role in the pseudogap phase of high-temperature superconductors.

Connection to the Haldane model. On the honeycomb lattice, the hopping term, analogous to Eq. (37) and leading to a chiral mass (Fig. 4), is

$$-i \frac{m_C}{4} \sum_{k,j=1}^{j=6} (-1)^j (\psi^\dagger_{R\mathbf{r}_k} \psi_{R\mathbf{r}_k+\mathbf{r}_j} - \psi^\dagger_{S\mathbf{r}_k} \psi_{S\mathbf{r}_k+\mathbf{r}_j}). \qquad (39)$$

The sum on k runs over all lattice sites in a given sublattice, and $\mathbf{r}_j$ are the six vectors which join a site and its next nearest neighbors. This construction is analogous to the Haldane model [56] for realizing conductance quantization in the absence of an external magnetic field in a honeycomb lattice. The contribution to the low-energy theory from this mass is the same as in the square lattice. In an experiment, the appropriate phases could be engineered through the use of light-assisted hopping, allowing the hopping elements to pick up local phases from an external laser beam [38].

D. Robustness

An important issue with our proposal is that of stability: How robust is our construction against symmetry-breaking perturbations? Inevitably, any realization of QED through this or a similar scheme must contend with anisotropies in the couplings, unequal or anisotropic Fermi and Bose velocities, and residual interactions which violate our emergent gauge invariance. Further, we have ignored the effect of the harmonic trapping potential required to confine the atoms; the long-ranged forces of QED could be disrupted if the trap were not shallow (although recent work has shown that stability of the Dirac points themselves are robust; see, for example [57,58]).

These are difficult issues, and we are unable at this point to quantify all of them. Each of these effects would have to be treated in detail, and their importance will inevitably hinge on technical details in the experiment. Some particular perturbations have been studied. For example, we have already seen that at low temperatures, QED3 is unstable toward

spontaneous chiral symmetry breaking. Near the transition temperature, small perturbations which break chiral symmetry can be quite important. Other perturbations are less destructive: For example, Vafek *et al.* [59] showed that anisotropy in the Fermi velocity is an renormalization group-irrelevant perturbation at low energies.

We do have some additional knowledge of the robustness of this model against Lorentz-invariant perturbations. Through a simple power counting, we argue that any generic Lorentz-invariant perturbation will have a vanishingly small contribution to the low-energy physics of our system. For this argument, we work in units with the dimensionality [energy] = [momentum] = [length]$^{-1}$ = [time]$^{-1}$ and label any quantity by the number of powers of energy that make it up. For example, energy will have dimension +1 and length dimension −1. By noting that the action must be dimensionless, the dimensionality of ψ is 1, and A is 1/2. According to the standard Wilsonian RG argument [30], only coupling constants with non-negative dimension will contribute to the low-energy physics. For example, mass terms and the gauge coupling e are relevant perturbations. Along with the Chern-Simons term and the fermion masses, the terms in the QED3 action (1) are the only relevant and marginal operators consistent with Lorentz and gauge symmetries that can be constructed from ψ and A fields.

V. (1 + 1)-DIMENSIONAL OPTICAL-LATTICE QED

We now discuss the (1 + 1)-dimensional analog to the model discussed in Secs. II and III.

The Feynman-gauge Hamiltonian for (1 + 1)-dimensional QED (QED2) is

$$H = \sum_k \overline{\psi}\gamma_1(v_F k + eA_1)\psi + \frac{1}{2}\partial_\mu A_\nu \partial_\mu A_\nu, \tag{40}$$

where ψ is a two-component fermionic spinor, A_ν are bosonic fields, $\nu = 0,1$, and $\gamma_1 = \sigma_y$. Following our previous arguments, one would expect this to be emulated by the (1 + 1)-dimensional generalization of our planar Hamiltonian (12),

$$\begin{aligned} H = &-t\sum_{\{x\in L_f, y\in L_b\}} \psi^\dagger_{R/S\downarrow x\pm\mathbf{l}}\psi_{S/R\downarrow x} + g_0\sum_x \psi^\dagger_{R/S\downarrow x}\psi_{R/S\downarrow x}n_{0x} + g_1''\sum_x \psi^\dagger_{R/S\downarrow x\pm\mathbf{l}}\psi_{S/R\downarrow x}n_{1\mathbf{y}=x\pm\mathbf{l}/2} + \sum_{b=0,1;k}\epsilon_{bk}n_{bk} \\ &+ \sum_{b=0,1;x}\frac{V_b}{2}n_{bx/y}(n_{bx/y}-1) + g_1'\sum_{\langle yx\rangle} a^\dagger_{1y+2\mathbf{l}}a_y(\psi^\dagger_{Sx}\psi_{Sx} + \psi^\dagger_{Rx+\mathbf{l}}\psi_{Rx+\mathbf{l}}) + \text{H.c.} + g_1''\sum_{\langle xy\rangle}\psi^\dagger_{R/Sx}\psi_{R/Sx}n_{1y=x\pm\mathbf{l}/2}. \end{aligned} \tag{41}$$

The lattice for this model is shown in Fig. 5. Here, the x represent fermion lattice sites (L_f), and the y represent the boson lattice sites (L_b) associated with every other bond between fermion lattice sites. ϵ_{bk} is the boson kinetic term and chemical potential, and it has a minimum at $K = \pi/2l$. Bosons of species a_0 are confined to the fermion lattice sites, and bosons of species a_1 occupy the **y** sites.

Unfortunately, the Hamiltonian in Eq. (41) does not yield QED2. While this Hamiltonian trivially has fermions with a Dirac dispersion, the boson-mediated fermion hopping term does not lead to a Bose-Fermi coupling of the form in Eq. (40). Instead, the resulting coupling, $e\overline{\psi}A_1\gamma_2\psi$, has an erroneous extra phase factor of $e^{i\pi/2}$ and violates Lorentz invarience. This same phase factor was also found in the two-dimensional (2D) case, but there it was benign: it simply meant that A_x is produced by bosons on the y bonds, and A_y is produced by bosons on the x bonds. In the one-dimensional (1D) case, however, we cannot make such a relabeling (since no γ_2 matrix appears in the fermion kinetic term). We can fix Eq. (41) by implementing additional phase factors into the mediated hopping matrix elements. Conceptually, the best way to implement these phases is to work in a larger space, allowing the fermions to hop onto the y sites, with a total energy cost of U relative to the x sites. Using the techniques from [21,23,36,38], one can engineer a spatially dependent phase on the hopping matrix elements and produce a Hamiltonian,

$$\begin{aligned} H = &-t\sum_{\{x\in L_f, y\in L_b\}} \psi^\dagger_{R/S\downarrow x\pm\mathbf{l}}\psi_{S/R\downarrow x} + U\sum_x \psi^\dagger_{\uparrow y}\psi_{\uparrow y} \\ &+ g_0\sum_x \psi^\dagger_{R/S\downarrow x}\psi_{R/S\downarrow x}n_{0x} + g_1\sum_x \psi^\dagger_{\uparrow y}\psi_{\uparrow y}n_{1y} \\ &+ \sum_{b=0,1;k}\epsilon_{bk}n_{bk} + \sum_{b=0,1;x}\frac{V_b}{2}n_{bx/y}(n_{bx/y}-1) + g_1' \\ &\times \sum_{\langle yx\rangle} a^\dagger_{1y+2\mathbf{l}}a_y(\psi^\dagger_{Sx}\psi_{Sx} + \psi^\dagger_{Rx+\mathbf{l}}\psi_{Rx+\mathbf{l}}) + \text{H.c.} + H_{\text{med}} \end{aligned} \tag{42}$$

$$H_{\text{med}} = \omega_t\sum_{\langle xy\rangle} e^{iQx}\psi^\dagger_{\uparrow y}\psi_{R/S\downarrow x} + \text{H.c.} \tag{43}$$

Here $\omega_t e^{iQx}$ is the matrix element for a fermion to hop onto a boson site, with $Q = \pi/2l$, and U is the onsite energy. Working

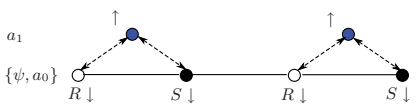

FIG. 5. (Color online) Lattice for the 1D theory, with sublattices labeled by spin and by the particles that inhabit them. Bold lines represent ordinary hopping terms and dashed lines indicate hopping facilitated by optical transitions, as described in the text.

to lowest nontrivial order in ω_t/U, we integrate out the y sites, obtaining

$$H_{\text{med}} = \frac{\omega_t^2}{U}\sum_x \left[(\psi^\dagger_{Rx+\mathbf{1}}\psi_{Sx}e^{iQx} + \psi^\dagger_{Sx}\psi_{Rx+\mathbf{1}}e^{-iQx}) \times \left(1+\frac{g_1}{U}n_{1y}\right) + \psi^\dagger_{R/Sx}\psi_{R/S}\left(1+\frac{g_1}{U}n_{1y}\right)\right], \quad (44)$$

which gives the desired low-energy Hamiltonian.

VI. 3 + 1 DIMENSIONS

Full $(3+1)$-dimensional QED can be simulated by combining the schemes which we have presented for one and two dimensions. We work with a cubic lattice formed by layering the 2D square lattice of Sec. III, with lattice spacing l_z between each layer. Each 2D layer is the same as the lattice of Sec. III, containing three bosons and one fermion distributed between the various sublattices. Between the layers we add a fourth boson species a_3, which occupies the space between every other layer and can only interact with the fermions through a light-assisted transition as in the 1D case. We then implement additional phases to change the sign of the hopping amplitudes t_z between planes; we choose the phases such that vertical hopping between sites on the R sublattice gets no additional phase but z-directional hopping matrix elements between sites on the S sublattices are opposite in sign. We ignore any vertical hopping beyond nearest neighbors. Under those conditions, our free particle Hamiltonian is

$$H = -2\sum_{\mathbf{k}} \psi^\dagger_{\mathbf{k}} M \psi_{\mathbf{k}},$$
$$M = \begin{pmatrix} t_z\cos k_z l_z & t\cos k_x l + it\cos k_y l \\ t\cos k_x l - it\cos k_y l & -t_z\cos k_z l_z \end{pmatrix}. \quad (45)$$

This Hamiltonian exhibits eight Dirac points, located at $\mathbf{k} = \pi\{\pm 1/2l, \pm 1/2l, \pm 1/2l_z\}$, though many of these are degenerate. We can obtain the necessary bispinor representation by simply combining pairs of them; for example, the combination of $\mathbf{K} = \pi\{1/2l, 1/2l, 1/2l_z\}$ and $-\mathbf{K}$ yields the following representation for the Lorentz group:

$$\Gamma_0 = \begin{pmatrix} 0 & 1_{2\times 2} \\ 1_{2\times 2} & 0 \end{pmatrix}, \quad \Gamma_j = i\begin{pmatrix} 0 & \sigma_j \\ -\sigma_j & 0 \end{pmatrix}. \quad (46)$$

The A_z component of the gauge field is derived from the a_3 bosons in the same manner as in Sec. V. Other than ensuring that the sign flips between sublattices are preserved when adding the gauge interaction, the derivation is essentially unchanged.

VII. SUMMARY AND OUTLOOK

We have proposed a number of experiments involving neutral atoms in optical lattices which will emulate the properties of relativistic quantum electrodynamics. These models are technically very difficult to realize, requiring a large number of lasers and atomic species that all must be fine-tuned to produce the desired behavior. However, the necessary technologies (optically induced phases, interpenetrating spin-dependent lattices, and tunable Bose-Fermi mixtures) for our model have all been separately realized in recent experiments. Further, as a weakly coupled route from a lattice model to a Lorentz-invariant thermodynamical gauge theory, the scheme we have proposed here is also of significant theoretical interest.

Finally, it would be interesting to establish whether this scheme could be extended to simulate more complicated gauge theories, such as non-Abelian theories or perturbative gravity. Given the importance of these theories in high-energy physics, a method for simulating them in cold atoms would be a very significant development. The difficulty of this process should not be underestimated. These theories intrinsically have a very large number of degrees of freedom; in $2+1$ dimensions, an SU(2) theory has nine gauge boson modes (three components of space-time with three SU(2) generators associated with each), and an SU(3) theory has twenty-four! Further, non-Abelian gauge theories have boson self-interactions that must be finely tuned to avoid breaking gauge invariance. Worse yet, the gauge fields exhibit ghostlike degrees of freedom with negative norm. Accounting for all of these effects in any scheme would be a daunting challenge. Nonetheless, quantum simulation of non-Abelian dynamical gauge theories is a fascinating prospect, and the theory we have described here could be an important first step in that direction.

ACKNOWLEDGMENTS

Eliot Kapit thank Andres LeClair, Liam Mcallister, and David Marsh for illuminating discussions related to this work. This work was supported by NSF Grant No. PHY-0758104, a grant from the Army Research Office with funding from the DARPA OLE program, and the Department of Defense (DoD) through the National Defense Science and Engineering Graduate (NDSEG) Program.

[1] S. Deser, R. Jackiw, and S. Templeton, Ann. Phys. **281**, 409 (1982).
[2] T. W. Appelquist, M. Bowick, D. Karabali, and L. C. R. Wijewardhana, Phys. Rev. D **33**, 3704 (1986).
[3] T. Appelquist, D. Nash, and L. C. R. Wijewardhana, Phys. Rev. Lett. **60**, 2575 (1988).
[4] I. J. R. Aitchison, N. Dorey, M. Klein-Kreisler, and N. E. Mavromatos, Phys. Lett. B **294**, 91 (1992).
[5] C. S. Fischer, R. Alkofer, T. Dahm, and P. Maris, Phys. Rev. D **70**, 073007 (2004).
[6] E. Dagotto, A. Kocić, and J. B. Kogut, Nuc. Phys. B **334**, 279 (1990).
[7] T. Appelquist, J. Terning, and L. C. R. Wijewardhana, Phys. Rev. Lett. **75**, 2081 (1995).
[8] M. Hermele, T. Senthil, and M. P. A. Fisher, Phys. Rev. B **72**, 104404 (2005).
[9] M. Hermele, Y. Ran, P. A. Lee, and X.-G. Wen, Phys. Rev. B **77**, 224413 (2008).
[10] I. J. R. Aitchison and N. E. Mavromatos, Phys. Rev. B **53**, 9321 (1996).

[11] D. H. Kim, P. A. Lee, and X.-G. Wen, Phys. Rev. Lett. **79**, 2109 (1997).
[12] M. Franz and Z. Tešanović, Phys. Rev. Lett. **87**, 257003 (2001).
[13] W. Rantner and X.-G. Wen, Phys. Rev. Lett. **86**, 3871 (2001).
[14] I. Bloch, J. Dalibard, and W. Zwerger, Rev. Mod. Phys. **80**, 885 (2008).
[15] E. Zhao and A. Paramekanti, Phys. Rev. Lett. **97**, 230404 (2006).
[16] L. B. Shao, S.-L. Zhu, L. Sheng, D. Y. Xing, and Z. D. Wang, Phys. Rev. Lett. **101**, 246810 (2008).
[17] C. Becker, P. Soltan-Panahi, J. Kronjäger, S. Dörscher, K. Bongs, and K. Sengstock, New J. Phys. **12**, 065025 (2010).
[18] P. Soltan-Panahi *et al.*, e-print arXiv:1005.1276v1.
[19] D. Poletti, C. Miniatura, and B. Grémaud, e-print arXiv:1006.3179v1.
[20] A. H. Castro Neto, F. Guinea, N. M. R. Peres, K. S. Novoselov, and A. K. Geim, Rev. Mod. Phys. **81**, 109 (2009).
[21] X.-J. Liu, X. Liu, C. Wu, and J. Sinova, Phys. Rev. A **81**, 033622 (2010).
[22] K. Osterloh, M. Baig, L. Santos, P. Zoller, and M. Lewenstein, Phys. Rev. Lett. **95**, 010403 (2005).
[23] S.-L. Zhu, B. Wang, and L.-M. Duan, Phys. Rev. Lett. **98**, 260402 (2007).
[24] D. Angelakis, M. Huo, E. Kyoseva, and L. C. Kwek, e-print arXiv:1006.1644v1.
[25] J. I. Cirac, P. Maraner, and J. K. Pachos, Phys. Rev. Lett. **105**, 190403 (2010).
[26] Y. Yu and K. Yang, Phys. Rev. Lett. **105**, 150605 (2010).
[27] L.-K. Lim, C. M. Smith, and A. Hemmerich, Phys. Rev. Lett. **100**, 130402 (2008).
[28] L.-K. Lim, A. Lazarides, A. Hemmerich, and C. Morais Smith, Europhys. Lett. **88**, 36001 (2009).
[29] M. P. Kennett, N. Komeilizadeh, K. Kaveh, and P. M. Smith, e-print arXiv:1011.1502.
[30] M. E. Peskin and D. V. Schroeder, *An Introduction to Quantum Field Theory* (Westview Press, Boulder, CO, 1995).
[31] P. A. Lee, N. Nagaosa, and X.-G. Wen, Rev. Mod. Phys. **78**, 17 (2006).
[32] B. A. Freedman and L. D. McLerran, Phys. Rev. D **16**, 1130 (1977).
[33] L. Dolan and R. Jackiw, Phys. Rev. D **9**, 3320 (1974).
[34] I. J. R. Aitchison, *An Informal Introduction to Gauge Field Theories* (Cambridge University Press, Cambridge, 1982).
[35] Y.-J. Lin, R. L. Compton, A. R. Perry, W. D. Phillips, J. V. Porto, and I. B. Spielman, Phys. Rev. Lett. **102**, 130401 (2009).
[36] Y.-J. Lin, R. L. Compton, K. Jiménez-García, J. V. Porto, and I. B. Spielman, Nature (London) **462**, 628 (2009).
[37] I. B. Spielman, Phys. Rev. A **79**, 063613 (2009).
[38] D. Jacksch and P. Zoller, New J. Phys. **5**, 56 (2003).
[39] A. Albus, F. Illuminati, and J. Eisert, Phys. Rev. A **68**, 023606 (2003).
[40] X.-G. Wen, *Quantum Field Theory of Many-Body Systems* (Oxford University Press, Oxford, UK, 2007).
[41] F. Ferlaino, C. D'Errico, G. Roati, M. Zaccanti, M. Inguscio, G. Modugno, and A. Simoni, Phys. Rev. A **73**, 040702 (2006).
[42] R. Jackiw and S. Templeton, Phys. Rev. D **23**, 2291 (1981).
[43] A. Bashir, A. Raya, I. C. Cloët, and C. D. Roberts, Phys. Rev. C **78**, 055201 (2008).
[44] H. Feng, W. Sun, D. He, and H. Zong, Phys. Lett. B **661**, 57 (2008).
[45] T. A. Corcovilos, S. K. Baur, J. M. Hitchcock, E. J. Mueller, and R. G. Hulet, Phys. Rev. A **81**, 013415 (2010).
[46] W. S. Bakr, J. I. Gillen, A. Peng, S. Fölling, and M. Greiner, Nature (London) **462**, 74 (2009).
[47] M. He, H. T. Feng, W. M. Sun, and H. S. Zong, Mod. Phys. Lett. A **22**, 449 (2007).
[48] S. Coleman and B. Hill, Phys. Lett. **159**, 184 (1985).
[49] Y. Hoshino and T. Matsuyama, Phys. Lett. B **222**, 493 (1989).
[50] B. M. Pimentel, A. T. Suzuki, and J. L. Tomazelli, Int. J. Theor. Phys. **33**, 2199 (1994).
[51] G. K. Campbell *et al.*, Science **313**, 649 (2006).
[52] J. Stenger, S. Inouye, A. P. Chikkatur, D. M. Stamper-Kurn, D. E. Pritchard, and W. Ketterle, Phys. Rev. Lett. **82**, 4569 (1999).
[53] J. Steinhauer, R. Ozeri, N. Katz, and N. Davidson, Phys. Rev. Lett. **88**, 120407 (2002).
[54] R. Ozeri, N. Katz, J. Steinhauser, and N. Davidson, Rev. Mod. Phys. **77**, 187 (2005).
[55] S. Chakravarty, R. B. Laughlin, D. K. Morr, and C. Nayak, Phys. Rev. B **63**, 094503 (2001).
[56] F. D. M. Haldane, Phys. Rev. Lett. **61**, 2015 (1988).
[57] J. K. Block and N. Nygaard, Phys. Rev. A **81**, 053421 (2010).
[58] L. H. Haddad and L. D. Carr, e-print arXiv:1006.3893.
[59] O. Vafek, Z. Tešanović, and M. Franz, Phys. Rev. Lett. **89**, 157003 (2002).